

# Muscle Synergy-Based Functional Electrical Stimulation Reduces Muscular Fatigue in Post-Stroke Patients: A Systematic Comparison

Smriti Bala<sup>1</sup>, Venugopalan Y. Vishnu<sup>2</sup>, and Deepak Joshi<sup>3</sup>, *Member, IEEE*

**Abstract**—Muscle synergy-based functional electrical stimulation had improved movement kinematics instantly and in long-term use in post-stroke patients. However, the therapeutic benefits and efficacy of muscle synergy-based functional electrical stimulation patterns over traditional stimulation patterns need exploration. This paper presents the therapeutic benefits of muscle synergy-based functional electrical stimulation compared to traditional stimulation patterns from the perspective of muscular fatigue and kinematic performance produced. Three stimulation waveforms/envelopes: customized rectangular, trapezoidal, and muscle synergy-based FES patterns were administered on six healthy and six post-stroke patients to achieve full elbow flexion. The muscular fatigue was measured through evoked-electromyography, and the kinematic outcome was measured through angular displacement during elbow flexion. The time domain (*peak-to-peak amplitude, mean absolute value, root-mean-square*) and frequency domain (*mean frequency, median frequency*) myoelectric indices of fatigue were calculated from evoked-electromyography. Myoelectric indices of fatigue and peak angular displacements of elbow joint were compared across waveforms. The presented study found that the muscle synergy-based stimulation pattern sustained the kinematic output for longer durations and induced less muscular fatigue followed by trapezoidal and customized rectangular patterns in healthy and post-stroke participants. These findings imply that the therapeutic effect of muscle synergy-based functional electrical stimulation stems from not only being biomimetic but also due to it being efficient in inducing less fatigue. The slope of current injection was a crucial factor

in determining the performance of muscle synergy-based FES waveforms. The presented research methodology and outcomes would help researchers and physiotherapists in choosing effective stimulation patterns for maximizing post-stroke rehabilitation benefits. **Note:** FES waveform/pattern/ stimulation pattern all refers to FES envelop in this paper.

**Index Terms**—Synergy-based functional electrical stimulation, muscle synergy, hemiparesis, elbow flexion, post-stroke rehabilitation, upper extremity, electrically evoked EMG, eEMG, FES-based exercises, dynamic contractions, muscle fatigue, myoelectric indices of fatigue.

## I. INTRODUCTION

STROKE is caused by a sudden disruption of blood supply in the brain that interferes with the affected region's function and task. The clinical manifestations include limb weakness or paralysis, loss of sensation, speech, hearing, vision, etc. Stroke is the second leading cause of death and disability worldwide [1]. Post-stroke paralysis has increased the global disability burden the most [2]. Whether ischemic or haemorrhagic, stroke-induced paralysis has the common adverse effects which includes limb weakness, learned non-use, and disrupted daily activities. Post-stroke rehabilitation is vital in helping survivors to lead normal lives since unused paralyzed limb muscles and joint movements deteriorate over time.

Physiotherapy improves paralyzed limb's biomechanics which can be further enhanced when combined with Functional electrical stimulation (FES) [3]. FES, which improves kinematic performance and reduces muscle wasting, has overcome this limitation by stimulating a non-functional limb. It restores movement in spinal cord injury [4], Parkinson's [5], cerebral palsy [6], and stroke [7] patients. FES reduces muscle degeneration during inactivity [8]. FES-induced repetitive exercises of single-joint movements like flexion and extension are of paramount importance in preventing joint-supporting muscle fiber degeneration and are used to treat SCI and stroke patients.

The outcomes of FES primarily depend on the envelope/waveform/stimulation pattern characteristics (*current amplitude, pulse width, and frequency*) [9]. FES waveforms targeting functional movements of joints use rectangular and trapezoidal envelope/stimulation patterns with various characteristics under clinical settings [9], [10]. The rectangular

Manuscript received 14 December 2022; revised 21 May 2023; accepted 23 June 2023. Date of publication 28 June 2023; date of current version 6 July 2023. This work was supported by the Prime Minister's Research Fellowship (PMRF) under Grant 1400069, Pln08/pmrf. (Corresponding author: Deepak Joshi.)

This work involved human subjects or animals in its research. Approval of all ethical and experimental procedures and protocols was granted by the Ethics Committee of All India Institute of Medical Sciences, Delhi, under Reference No. IEC-299/07.05.2021.

Smriti Bala is with the Centre for Biomedical Engineering, Indian Institute of Technology Delhi, New Delhi 110016, India (e-mail: bms188298@iitd.ac.in).

Venugopalan Y. Vishnu is with the Department of Neurology, All India Institute of Medical Sciences, New Delhi 110029, India (e-mail: vishnuvy16@yahoo.com).

Deepak Joshi is with the Centre for Biomedical Engineering, Indian Institute of Technology Delhi, New Delhi 110016, India, and also with the Department of Biomedical Engineering, All India Institute of Medical Sciences (AIIMS), New Delhi 110029, India (e-mail: joshid@iitd.ac.in).

This article has supplementary downloadable material available at <https://doi.org/10.1109/TNSRE.2023.3290293>, provided by the authors. Digital Object Identifier 10.1109/TNSRE.2023.3290293

stimulation waveform combines a small increasing ramp followed by a constant stimulation intensity. A trapezoidal stimulation pattern is formed using ramp-up, rectangular, and ramp-down signals, more like rise, hold, and fall. These FES envelopes/patterns are used to induce joint movements and are commonly delivered by clinicians [11]. The absence of a common consensus over stimulation protocols (*specifically FES patterns*) results in variations in rehabilitation outcomes such as Fugl Meyer scores.

Muscle fatigue, a serious concern induced by FES that restricts therapy duration and diminishes the full benefits of FES [12], also vary under different traditional/conventional (*as per previous works*) waveforms [13], [14]. Additionally, these conventional waveforms are unguided, i.e., not inspired and derived from neural control of movements, and thus may not be efficient for restoring the movements. Recently, muscle synergy-driven FES waveforms have been shown to be efficient in restoring muscle functions in stroke patients [15].

The main objective of using muscle synergy-based FES in recent FES paradigm is to solve the perpetual issue in FES [16], that is how to optimize the pattern of multiple channels of stimulation in rehabilitation regimen, to induce the maximal positive reorganization of brain motor system to offset the damaged functions [16]. The muscle synergy-based FES provides an FES initiation template which is proposed as a solution because it follows the similar organization of biological motor control [16], [17]. The study of Niu et al. [15] has illustrated the acute benefits of synergy-based FES. An investigation into an automated accelerometer-triggered synergy-based FES [18] and a recent randomized clinical trial (RCT) by Niu et al. [19] on the similar protocol [15] has demonstrated the short-term efficacy of synergy-based FES with a 5-day intervention on post-stroke patients.

However, these studies are limited to being assessed by only functional outcomes using kinematic data. These functional outcomes have not been associated with muscle fatigue so far. FES-induced fatigue is a serious concern when considering stroke rehabilitation. Therefore, it is important to investigate the muscle synergy-based FES waveform in association with functional outcome as well as muscle fatigue. In contrast to previous work using various stimulation waveforms [20], [21], [22], [23], where only functional outcomes were investigated, the authors believe this to be the first study that considers muscle fatigue as an assessment for the efficacy of muscle synergy-driven FES waveform for post-stroke rehabilitation.

In addition, the present work utilizes an improved method to choose a synergy template to generate the waveform of FES for doing elbow flexion, a crucial single joint upper extremity movement that helps in lifting tasks. In the previous approaches, the muscle synergy templates have been utilized by using the electromyography (EMG) signal of an age-matched healthy individual [15]. However, in the present work, rather than age-matched, an objective assessment of intra-subject and inter-subject similarity of muscle synergies while doing a specific task (*including the nonparetic limb of post-stroke and dominant limb of healthy individuals*) was utilized to select the muscle synergy template. Such a method being

biomimetic [24], develops a hypothesis that the fatigue will be minimized by this template-driven FES. Hence, it can be hypothesized that the increased kinematic outputs, such as peak velocity and improved functionality, with instantaneous use of synergy-based FES in past work [15] could have been due to the reduction in one of the most important concerns of FES, i.e., stimulation-induced muscle fatigue. Hence in this study, the results on both functional performance and muscle fatigue from synergy-driven FES are compared with that of conventional methods of stimulation that are: rectangular and trapezoidal waveforms/envelopes.

The primary challenge while assessing muscle fatigue from evoked electromyography (eEMG) through myoelectric indices (*these are time and frequency domain features calculated on evoked EMG*) is the stimulation artifact. Various approaches are proposed in the literature to minimize the artifacts in eEMG. The main approaches include the blanking window method [25], comb filter [26], bandpass-comb filter [27], and empirical mode decomposition (EMD) based filtering [28]. The present work also investigates the effect of these filtering methods and suggests the optimal filtering technique for the present application.

The significant contributions of present work are:

a) Combined assessment of kinematic performance and muscle fatigue on elbow joint flexor muscles using muscle synergy-based and conventional FES pattern. Here, peak angular displacement of elbow joint (*measured from electronic goniometer*) and myoelectric indices (*calculated from eEMG*) are the indicators of kinematic performance and muscle fatigue. b) An effective, biomimetic, synergy-based FES template is developed based on intra- and inter-subject similarity in muscle synergies. Task-specific (*elbow flexion*) muscle synergies were compared across the participants to select the FES driving template. c) Comparison of eEMG artifact filtering schemes is done since artifact removal in unprocessed eEMG helps estimate accurate myoelectric indices. Different artifact-removal techniques filter the signal differently. Myoelectric indices results are affected by filtering. Hence, the choice in the filtering scheme is presented.

## II. METHODS

### A. Stimulation Parameters

*a. Stimulation pulse amplitude and pulse width:* Maximum angle of elbow flexion was used to determine the stimulation current level. It was determined by giving ramp-patterned stimulation at 200  $\mu$ s [29], [15] pulse width and 40 Hz frequency to both biceps brachii and brachioradialis simultaneously for full flexion. *B. Stimulation frequency:* Pulse frequencies between 20 to 50 Hz [30] are the standard treatment for post-stroke paralysis. FES applications prefer tetanic contraction [30], hence 40 Hz pulses are needed [29], [30]. So, 40 Hz stimulation frequency was chosen. *C. Pulse shape:* Symmetric biphasic pulses were chosen so that charge stored in the tissues (*which is detrimental*) would be eliminated in the negative part of the pulse [30]. *D. Singlet/doublet/triplet:* Muscles twitch with each electric pulse. If the next stimulation pulse is administered before the muscle relaxes, additional twitches will occur. Each twitch adds up to a mean force

greater than a single twitch [30]. N-let (*N- double, triple*) pulses provide more force. This study used doublet stimulation pulses on recommendations [31], [32].

### B. Lab System Software

1) *Stimulation Patterns*: The first two conventional stimulation patterns, customized rectangular (*W1*) and trapezoidal (*W2*), were constructed utilizing existing procedures for flexion/extension protocols on stroke and spinal cord injury patients. Protocols for spinal cord injury patients were included because stroke and SCI patients experience FES-induced muscle fatigue. However, in literature, many variations in terms of ramp time, stimulation duration, receding slope, type of extremity, muscle of application, and functional activity exist for these two conventional stimulation patterns: rectangular (*W1*) [23] and trapezoidal (*W2*) [29], [33]. Therefore, traditionally used stimulation pattern characteristics were modified to achieve upper limb maximum angle of elbow flexion. This study's third stimulation pattern was muscle-synergy-based FES (*W3*).

2) *Steps to Create Stimulation Patterns*: i. Customized Rectangular stimulation pattern (*W1*) formulation steps: This stimulation pattern was like trapezoidal; however, it just has a ramp up before maximum intensity [23]. The customized rectangular stimulation patterns had an 8s ramp up (*to prevent high-current shock*) and 2s hold. Quick ramp up to peak current amplitude caused unsmooth angular displacements in preliminary experiments, hence, an 8s ramp up was found apt and was used.

ii. Trapezoidal stimulation pattern (*W2*) formulation steps: The trapezoidal stimulation patterns used for stimulating upper extremity joints have different protocols such as a general rise and fall time of 2s with 8s on and 6s off periods where ramp portion can vary between 0.1s to 6.5s [20]; a ramp and fall time of 3s [21]; a ramp-up of 0.1s and fall of 2s with 5s contraction time [34]; etc. In this study an 8s ramp up and 8s ramp down were chosen with a peak current hold time of 2s for a symmetric trapezoidal stimulation pattern.

iii. Muscle-synergy-based stimulation pattern (*W3*) formulation steps [15]: Voluntary activity of elbow flexion and extension i. e., biceps curls were used to create synergy-driven FES.

### C. Choice of Muscle Synergy From Available Templates for FES Stimulation Pattern

Previous work on synergy-driven FES for multi-joint activity chose a healthy female participant who was 54 years old [15]. However, for single-joint or multi-joint movements, it is still an open-ended question as to whose muscle synergy template could be used, and whether a difference could occur while choosing a particular muscle synergy template? This further led to an important query -instead of choosing the best template or, say, a universal template, could the post-stroke participant's healthy limb's synergy be used to drive the FES. To address this, the muscle synergies of 7 different persons (*6 healthy and 1 post-stroke participants*) were calculated who continuously performed the elbow flexion and extension

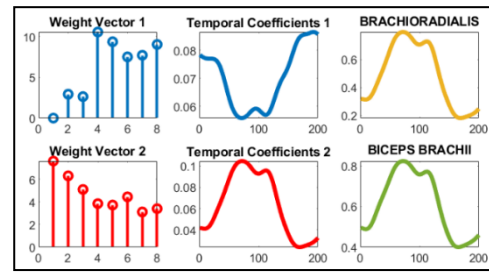


Fig. 1. Chosen muscle synergy of a healthy individual S6. Two optimum synergies were obtained after non-negative matrix factorization. The product of weight vectors and temporal coefficients gives reconstructed EMG of Brachioradialis and Biceps Brachii muscles.

activity for 20 cycles. The healthy participants performed the activity with their right dominant limb while the 57-year-old post-stroke participant performed the activity with his non-paretic limb). The healthy participants consisted of 5 young male adults aged ( $30.25 \pm 2.21$  years) and 1 age-matched spouse of the post-stroke patient (*55-year-old, female*). The choice of subjects was restricted to a smaller number as it would add many variables and factors to the study which would be a diversion to the present work. EMG from elbow flexion-extension activity was recorded from the following muscles: biceps brachii, brachioradialis, brachialis, triceps long head, triceps short head, anconeus, deltoid anterior, and deltoid posterior.

Steps to extract muscle synergies per participant were followed from here [35], EMG signals were recorded for 20 elbow flexion-extension cycles (*one cycle included flexion and extension*). The recorded EMG signals were band-pass filtered at 30–400 Hz (*zero lag 4<sup>th</sup> order Butterworth*), full wave rectified, and low-pass filtered at 6 Hz (*zero lag 4<sup>th</sup> order Butterworth*). To ensure that the muscle-specific EMG linear envelopes remained within the range of 0 to 1, they were normalized by the highest values found across the processed cycles. Each of the linear envelopes which reflected the muscle activation pattern was then reduced to 200 data points and interpolated using cubic splines. Data matrices with the number of rows representing the muscle activation patterns and the number of columns representing the number of data points (*i.e., 8-by-200*) were created. Muscle activation patterns for each participant were arranged into an 8-by-200 ( $200 \times 20$ ) matrix, where 200 represented the data points of a cycle, 8 represented the number of measured muscles, and 20 represented the total number of cycles. The muscle synergies were extracted from the developed matrix using non-negative matrix factorization [15] at 80% variance accounted for (*VAF*) [36]. The number of synergies could vary anywhere between 1 to total number of muscles. NNMF was repeated 25 times at each synergy level and the one with least residue was chosen. The number of synergies were not increased if the VAF increment was  $<5\%$  upon addition of new synergy. In this process the number of optimum synergies [36] for elbow flexion-extension activity were either one, two, or three as observed in all participants. The muscle synergies of 6 healthy subjects and one stroke subject's non-paretic hand have been shown in supplementary Fig. a (*S1-S7*). The types of synergy

patterns investigated in this study were not identical for all the individuals even at a particular condition (*supplementary Fig. a.*). Age, gender, % of maximum voluntary contraction while doing the activity, hand dominance, fatigued and non-fatigued state are some of the most important factors that could affect the muscle synergy and muscle synergy driven FES's outcomes. Hence, the participant exhibiting the most inter-cycle similarity and the highest synergy similarity with other participants was chosen as the most-suited synergy template irrespective of gender and age as shown in Fig. 1. Intra-subject variability was examined by first establishing muscle synergies across trials for each subject. Next, the cosine similarity of synergy vectors (SSV) was determined by using the formula [37]:

$$SSV(W_i^k, W_j^k) = \frac{W_i^k \cdot W_j^k}{\|W_i^k\|_2 \cdot \|W_j^k\|_2} \quad (1)$$

where  $W_i^k$  is the synergy vector from the  $i^{\text{th}}$  repetition and  $W_j^k$  is the synergy vector from the  $j^{\text{th}}$  repetition. An SSV value can be anywhere between 0 and 1. The greater the SSV, the closer the two vectors are. In addition, the cosine similarity of the synergy matrix (SSM) was found, which was the average of synergy vector similarity between any two synergy vectors from two synergy matrices, using the formula [37]:

$$SSM(W_i, W_j) = \text{mean} \left( \sum_m \sum_n \frac{W_i^m \cdot W_j^n}{\|W_i^m\|_2 \cdot \|W_j^n\|_2} \right) \quad (2)$$

where  $W_i^m$  and  $W_j^n$  are the  $m^{\text{th}}$  and  $n^{\text{th}}$  synergy vector of synergies  $i$  and  $j$  respectively. The most-suited synergy was chosen as the synergy extracted from healthy individual S6 for showing the most intra- and inter- subject similarity. The extracted synergies were used for EMGs reconstruction [15]. The reconstructed EMG envelopes were rescaled to time-amplitude domain and processed with concatenated piecewise-linear approximation.

#### D. Mapping Synergy-Based Reconstructed EMG to FES

The shape of the reconstructed EMG was translated to FES stimulation pattern using an inverse estimation method. Subject S6, whose muscle synergy template was chosen, was given different FES ramp signals (*+slopes*) and trapezoidal signals (*of different rising and falling slopes*) and the resultant eEMG signals were recorded. Stimulation artifacts were removed from eEMG using empirical mode decomposition. The filtered eEMG was low pass filtered with 4<sup>th</sup> order zero phase shift Butterworth filter at 6 Hz cut off frequency to obtain the envelop of eEMG. The obtained envelop was piecewise linearized using approximations to obtain straight lines with a characteristic slope. The slopes of eEMG envelop were in mV/s whereas the corresponding FES patterns were in mA/s. A calibration curve was obtained which was used to find stimulation pattern slopes corresponding to the reconstructed EMG of subject S6. It was assumed that eEMG envelop should mimic the reconstructed EMG envelop which was obtained from muscle synergies. Thus, stimulation pattern slopes were found using an inverse estimation method. This

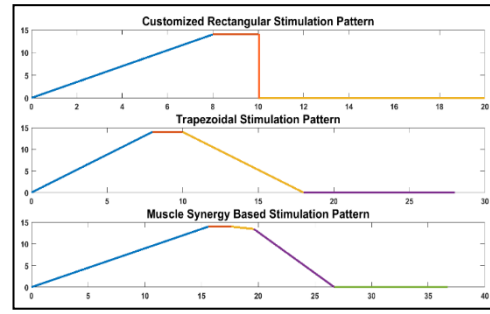


Fig. 2. This figure shows all the stimulation patterns used for stimulation. The first stimulation pattern is a customized rectangular stimulation pattern with an initial ramp-up stage followed by a 2s hold duration; the second is a trapezoidal stimulation pattern with equal ramp-up and ramp-down time, it too contained a 2s peak stimulation hold time, while the third one is a muscle-synergy-based stimulation pattern which also contained a 2s peak stimulation hold time followed by a two-tier decreasing pattern.

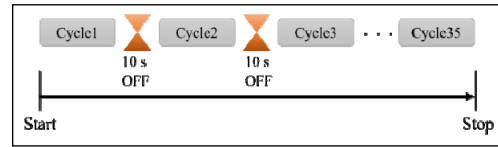


Fig. 3. This figure shows the protocol followed in every session. There was a total of 35 cycles recorded. Between the two cycles there was a 10 s off period.

way the synergy-based stimulation template was formed. The envelop corresponding to biceps brachii and brachioradialis were used as stimulation profiles for stimulating biceps brachii and brachioradialis muscle of participants. All stimulation patterns for a typical participant are shown in Fig. 2 and the experimental protocol is shown in Fig. 3.

#### E. Lab System Hardware and Stimulation Protocol

The experiment tested muscle fatigue from cyclic stimulations under different patterns. During the experiment, FES-evoked EMG data were captured using DELSYS Trigno Wireless EMG sensors at 2000 Hz, and elbow angle was measured using a goniometer and data recorder (*Biometrics Ltd., UK*) at 2000 Hz. Both systems were synchronized using DELSYS Trigger Module. Hair removal and ethanol cleaning prepared the skin for electromyography sensors and goniometer. A set of elbow flexions was recorded with a 10-second inter-cycle break (*protocol in Fig. 3*). No fatigue-inducing techniques (*such as little or no intermittent rest intervals*) were used. Electrical stimulations were provided using Hasomed RehaStim2 only to the elbow flexor muscles. Two pairs of RehaTrode FES electrodes, oval-shaped in size 4 by 6.4 cm, were utilized to stimulate two muscles (*biceps brachii and brachioradialis*). FES stimulation patterns parameters were controlled by MATLAB 2019 b version. The experimental setup with the participant is shown in Fig. 4.

#### F. Experimental Paradigm

The activity of elbow flexion in vertical plain (*Fig. 5*) is an important single joint activity of elbow joint. This activity improves strength of the elbow flexor muscles and

TABLE I  
SUBJECT DESCRIPTION

Sub Id	Affected Side	Age	Gender	Hand Dominance	Type of stroke	Implications other than Paralysis	Fugl-Meyer Scores (UE)#	Additional Information	Occurrence of stroke	Maximum current injected (mA)
P1	Right	64	Male	Right	Ischemic	Speech loss	24	Flaccidity	< 2 months	32.5
P2	Right	57	Male	Right	Ischemic	Speech loss	28	Flaccidity	<3 months	26.5
P3	Right	62	Male	Right	Hemorrhagic	NA	30	Flaccidity	6 months	24
P4	Right	58	Male	Right	Ischemic	Tremor	32	Spasticity	6 months	29
P5	Right	65	Male	Right	Ischemic	NA	34	Spasticity	<6 months	27
P6	Right	62	Male	Right	Ischemic	NA	36	Spasticity	<5 months	25
H1-H6	NA	26.8±1.78	Male	Right	NA	NA	NA	NA	NA	10.5, 21.48, 18.75, 20.75, 14.75, 22.25

P1-P6 denotes post-stroke subjects, H1-H6 denotes healthy subjects. # Fugl Meyer score [40] is applicable to all ages who have suffered stroke. 66 is the maximum score achieved for upper extremity (UE). Patients with severe joint contractures were avoided for the study, as joint movement is restricted to perform functional activity. NA represents 'not applicable'.

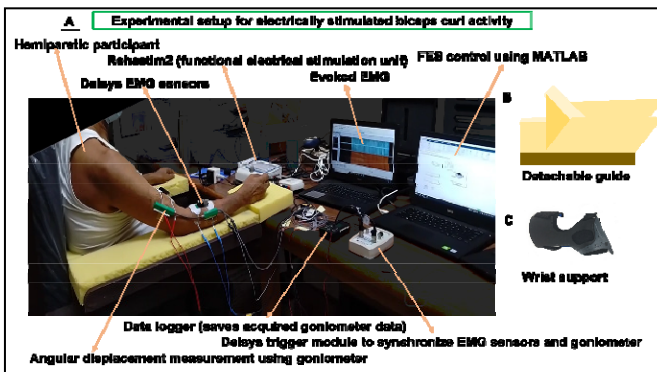


Fig. 4. Shown in the above figure is a hemiparetic post-stroke participant. The measurements of surface EMG signals from biceps brachii and brachioradialis have been time synchronized by Delsys trigger module. The synchronous pulses and the pattern of stimulation were controlled by MATLAB 19b version.

#### Single-joint Elbow Flexion

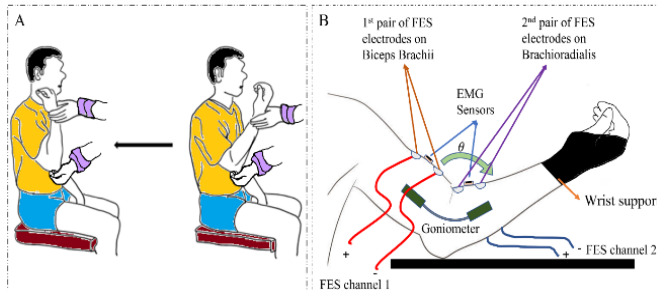


Fig. 5. A. The figure shows the manual intervention performed by a physiotherapist to improve the elbow flexion activity. Fig. 5. B. shows the same activity performed with an intervention of FES.

helps in improving lifting tasks, for example drinking, eating, picking objects etc. The traditional paradigms involve either stimulating biceps brachii alone [38] or biceps brachii and brachioradialis both [39]. It was observed from preliminary observations (illustrated in Table A in supplementary) that stimulating both biceps brachii and brachioradialis lowers the maximum current requirement for achieving full flexion. This study is based on comparisons of various stimulation patterns used under previously followed experimental paradigms, hence

conventionally used muscles (*biceps brachii* and *brachioradialis*) were the muscles that were being stimulated.

#### G. Participants

Six post-stroke male individuals with right-sided hemiplegia were chosen from sub-acute phase since significant improvements in functionality is observed in the sub-acute phase [41]. During initial screening of participants, the left hemiplegic and women participants did not accord to the inclusion criteria due to their conditions and various medical factors. Post-stroke participants (P4-P6) displayed mild spasticity (*Modified Ashworth Scale, MAS=1*) in wrist and fingers extensor muscles, which is safe for FES application [42] in the current study. Six healthy people also participated in the experiments as explained by the last row of Table I. The study examined the effect of FES pattern type on muscular fatigue, so, participant's age wasn't made a constraint. Ethical clearance for these experiments was approved by the All India Institute of Medical Sciences ethics committee (Ref. No. IEC-299/07.05.2021). Consent of voluntary participation in the research was taken from each participant.

#### H. Experimental Procedure

The individuals sat in a post-stroke chair built for comfort. The injured limb was put on a cushioned broad chair handle. The hand was supported by detachable guiding wedges and wrist joint support as shown in Fig. 4 B and C. Fugl-Meyer scores for post-stroke participants were calculated before intervention which is mentioned in Table I. Biceps brachii (BB) and brachioradialis (BR) muscles were stimulated simultaneously. Spasticity and flaccidity levels have been assessed under the expert's guidance, categorizing them as mild, moderate, and severe.

Prior to the FES session, each participant's pain and motor thresholds were assessed using an increasing ramp signal given to both flexors simultaneously at 200 $\mu$ s pulse-width, 40 Hz frequency, and doublet biphasic symmetric pulses. The peak sustainable current to produce complete flexion was determined from this activity. Table I shows all peak injectable current values. To ensure safety, the current injection

was constrained to 35 mA. The experiment was divided into three sessions, where each session corresponded to one type of stimulation pattern. Before the start of the session three integers 1, 2, 3 were generated randomly using MATLAB to remove any bias associated with the order in which stimulations were given. The generated random integers determined the order and type of stimulation pattern. Integers 1, 2, and 3 corresponded to customized rectangular, trapezoidal, and synergy-based stimulation patterns. Participants were made familiar with experimental techniques but not the stimulation patterns.

Since post-stroke patients were in sub-acute phase and were receiving FES for the first time, at least 35 cyclic motions were targeted in each session. After each stimulation pattern, a 1 hour 30 minutes pause was given to wear off the effect of muscle fatigue. Electrodes and sensors were switched off but not removed between sessions to ensure the same placement. The position of the muscles belly, EMG sensors placement, FES electrodes placement was followed according to standard protocols of practice under the expert's guidance. The parameters and the waveform/envelope were pre-loaded in the 'Signal Builder' block of the Simulink interface which controlled Rehasim2. Each target muscle's belly was attached to a pair of electrodes which were spaced apart by about 20 mm.

### I. Movement Tasks

The functional activity was to position the arm on the customized chair so that the resting forearm was set to a 0-degree reference angle. Activating biceps brachii and brachioradialis simultaneously flexed the elbow in vertical plane. In patterns W2 (*trapezoidal*) and W3 (*synergy-based*), elbow extension was partially regulated by receding biceps brachii and brachioradialis stimulation intensity. The activity involved is shown in Fig. 5. The goal was to achieve maximum angle of elbow flexion in an individual.

### J. Signal Processing and Data Analysis

The experimentally acquired angular displacement signals and electrically evoked electromyography (*eEMG*) were affected by noise and stimulation artifacts.

1) *Kinematic Data Filtration*: The goniometer data was filtered using the 3<sup>rd</sup> order Butterworth filter at 10 Hz cut-off frequency to remove high frequency noise.

2) *Evoked EMG Filtration*: The Electrically evoked EMG (*eEMG*) which contained the M-waves were contaminated by stimulation artifacts whose magnitude was several times higher than that of the M-waves [28] (*as shown in supplementary Fig. b*). Works in past, blanked EMG signals during stimulation using additional circuits, but commercial sensors lack peripheral circuitry compatibility. Hence, denoising of stimulation artifacts often use comb filters [26], online blanking window [43], adaptive filters [44], empirical mode decomposition methods [28] etc. Like blanking circuits, program-based blanking windows replace all stimulation artifact values with 0s. But even a small mismatch of data points between the stimulation artifact and the overlapping blanking window can

cause incomplete suppression of artifacts. This means that some artifacts may still be present if the blanking window does not overlap accurately with the stimulation artifact. To reduce these inaccuracies, other filtering schemes are used. A comparison of filtered *eEMG* obtained from using various filtration techniques is figuratively represented in the supplementary material Fig. b. The energy of filtered *eEMG* (*sum of eEMG magnitude-squared, i.e.,  $\sum_{i=1}^{i=N} |eEMG|_i^2$* ) from various filtration methods was compared against the energy of the envelop of raw *eEMG*, to understand which filtration method preserved most of the signal content. The envelop of raw *eEMG* was obtained from a low pass filtered version of a raw *eEMG* signal at 4 Hz with zero phase lag 4<sup>th</sup> order Butterworth filter. Low pass filtering removed stimulation artifacts from raw *eEMG*. The method utilized in this study to filter *eEMG* was empirical mode decomposition (*EMD*) [28] since its energy content was closest to the *eEMG* envelope.

### K. Parameters of Outcome Measure

1. *Kinematic performance estimator* (maximum joint angle)- For exercise-based cyclic (*repetitive*) FES programs which consist of intermittent breaks to avoid fatigue, torque decline [45] and joint angle decline [46] are evaluated as estimators of fatigue. Since fatigue caused by FES is an instantaneous performance deterrent, its effect persists and accumulates throughout the session. Therefore, fatigue was measured by a decline in peak angular displacements over cycles, which served as the primary measure to assess both performance and fatigue effects due to stimulation.

2. *Myoelectric indices of fatigue*- Frequency domain features (*mean frequency (MNF)*, *median frequency (MDF)*), and time domain features (*peak-to-peak amplitude (PTP)*, *mean absolute value (MAV)*, and *root mean square (RMS)*) of *eEMG* are known as myoelectric indices of fatigue. Decline in peak values of myoelectric indices over cycles were used as secondary estimators of fatigue. The myoelectric indices are well pronounced in isometric contractions for fatigue estimations [47], [48], but for dynamic intermittent contractions these indices are not firmly established [49]. However, median frequency (*MDF*) was found to be an effective fatigue estimator in FES-induced dynamic contractions [50]. Additionally, peak-to-peak amplitude (*PTP*), a time domain feature, was associated to joint angle during dynamic contractions for fatigue estimation with reliable results [51], [52]. The same could be observed for mean absolute value (*MAV*) feature in past works [53]. Therefore, mean frequency (*MNF*), median frequency (*MDF*), peak-to-peak amplitude (*PTP*), mean absolute value (*MAV*), and root mean square (*RMS*) were investigated as myoelectric indices of fatigue.

### L. Steps to Estimate Myoelectric Indices From *eEMG*

The steps to extract *MNF*, *MDF*, and *RMS* could be found here [54], *PTP* here [51], and *MAV* here [43] as well as in the supplementary Fig. d. The *EMD* filtered *eEMG* signal of each cycle was divided into epochs of 0.5 second window. The myoelectric indices of fatigue (*MNF*, *MDF*, *MAV*, and *RMS*) were extracted from these windows. These windows had an

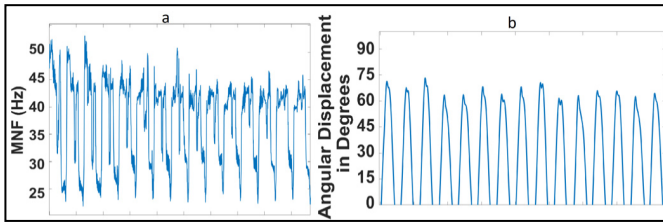


Fig. 6. (a) Mean frequency (MNF) (restricted to 15 cycles for visualization) and (b) angular displacements (restricted to 15 cycles for visualization) evoked during customized rectangular stimulation pattern of a particular subject.

overlapping of 25%. Peak-to-peak amplitude was calculated for each M-wave present in a particular cycle. The data from the break period was not used for any feature extraction. Similarly, for angular displacements post filtration the resting period data was removed for further cycle-wise analysis. A representation of MNF and angular displacements cycle-wise is shown in Fig. 6.

#### M. Trend Analysis of Parameters of Outcome Measure

Since the myoelectric indices were cyclically repetitive in nature just like joint angular displacements (as shown in MNF part of the Fig. 6) the trend of indices was estimated using peak values of indices per cycle. The indices were smoothed by using a moving average filter of 10 samples at first before finding the peak values. Then the peak values of all cycles of a fatigue index, such as mean frequency (MNF), were linearly fitted to get the trend. These trends give slope values which were treated as secondary estimates of fatigue in this study. For example, a negative slope value of the trend of mean frequency indicated a progressive decline in the peak feature value with cycles, indicative of fatigue. The process to obtain the slope of a fatigue index was figuratively illustrated in supplementary Fig. f and Fig. g. Similarly, the rate of change of kinematic output was calculated from linear fitting all the peak angular displacement value per cycle.

#### N. Statistical Analysis

Normality of data was examined with Shapiro-Wilk test. The following hypotheses were tested at statistical significance level of  $p < 0.05$ .

##### Part 1 Myoelectric Indices of Fatigue

The Kruskal Wallis test was performed to study the effect of different stimulation patterns on myoelectric indices of fatigue for every individual participant. Pairwise comparisons W1-W2, W2-W3, W1-W3 were performed to locate the differences. Friedman One-Way Repeated Measure Analysis of Variance by Ranks was performed to study the effect of different stimulation patterns on peak values of myoelectric indices for every individual participant. Pairwise comparisons W1-W2, W2-W3, and W1-W3 were performed to see where the differences lied. The statistically significant difference in rate of change of peak myoelectric indices (*slopes of peak myoelectric indices*) under different stimulation patterns in healthy and post-stroke participants was examined through

the Kruskal Wallis test. This included intra- and inter-group comparisons.

##### Part 2 Kinematic Performance Estimator

Repeated Measures One-way ANOVA was performed to study the effect of different stimulation patterns on peak angular displacements for every individual participant. Pairwise comparisons W1-W2, W2-W3, and W1-W3 were performed using post-hoc test to see where the differences lie.

The experimental design consisted of two groups-healthy and post-stroke. The Kruskal Wallis test was performed on slope values of peak angular displacement under different stimulation patterns in healthy and post-stroke groups. This included intra- and inter-group comparisons.

Note: All pairwise comparisons (W1-W2, W2-W3, W1-W3) in the above analyses were done with the Bonferroni correction method with  $p\text{-value} = 0.0167$  (which comes from  $\alpha/3$ ,  $\alpha$  is 0.05, here  $\alpha$  is the level of significance).

### III. RESULTS

#### Part 1 Myoelectric Indices of Fatigue

##### A. Statistical Analysis

We examined whether the myoelectric indices of fatigue generated under different stimulation patterns in any subject were identical. Subject-wise hypothesis testing was done since no two subjects have identical physiology; also, myoelectric indices of fatigue were hypothesized to be dependent on stimulation current (Table I). The myoelectric indices of fatigue (MNF, MDF, PTP, MAV, and RMS) were non-normally distributed as tested by the Shapiro-Wilk test, hence, were compared by Kruskal Wallis test across three waveforms/stimulation patterns. There were statistically significant differences ( $p < 0.05$ ) in the myoelectric indices of fatigue across the three tested stimulation patterns W1(customized rectangular), W2(trapezoidal), and W3(muscle synergy-based), indicating that the evoked EMG varied significantly under different waveforms for the same elbow flexion activity. Pairwise comparisons (W1-W2, W2-W3, W1-W3) were performed for all subjects and all myoelectric indices revealing statistically significant differences ( $p < 0.0167$ , Bonferroni corrected). There were few instances in which insignificant differences ( $p > 0.0167$ , Bonferroni corrected) were observed between pairs, but about 8 percent of all cases (30 out of 360 p-values of tested instances) were in this category. These 30 cases occurred randomly and did not produce inference (*all p-values in supplementary Table B*).

#Note: 12 subjects \* 2 muscles \* 5 myoelectric indices \* 3 pairs of stimulation patterns give 360 p-values

Additionally, the non-normally distributed peak values of myoelectric indices were also significantly different ( $p < 0.05$ , Friedman One-Way Repeated Measure Analysis of Variance by Ranks [55]) across the different stimulation patterns in all subjects. W1-W3 and W2-W3 pairs were significantly different ( $p < 0.0167$ , Bonferroni corrected) unlike W1-W2 which displayed many instances of insignificant differences (*all p-values in supplementary Table C*).

Within the post-stroke group, comparisons on the slope values of myoelectric indices across the three different waveforms

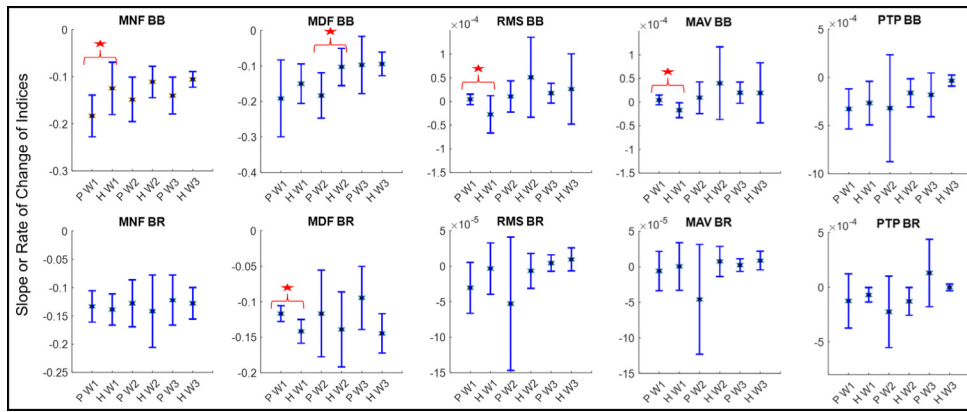


**Fig. 7.** The figure shows the average  $\pm$  standard deviation in slope values of myoelectric indices of fatigue observed for healthy and post-stroke participants in two muscles: biceps brachii and brachioradialis under three different stimulation patterns. The figure depicts the inter group comparison of healthy and post-stroke under three distinct stimulation patterns. BB and BR stand for biceps brachii and brachioradialis respectively; P and H stand for Post-stroke and Healthy; W1, W2, W3 are the waveforms. MNF, MDF, RMS, MAV, and PTP are the five myoelectric indices of fatigue. The red stars show the significant difference observed between both the groups measured using the Kruskal Wallis Test,  $p < 0.05$ . The figure depicts that the waveform W1 causes observable significant differences between healthy and post-stroke implying that waveform W1 is population sensitive even under a small sample size.

(Fig. 7, significant differences highlighted in green color) revealed significant difference ( $p < 0.0167$ , Bonferroni corrected) between W1 and W3 in mean frequency for biceps brachii muscle. However, within the healthy group no significant differences were observed in slope values of myoelectric indices across different stimulation patterns.

In inter-group comparisons (Fig. 7, significant differences highlighted in red color), the slope values of myoelectric indices were compared between post-stroke (P) and healthy (H) groups using the Kruskal Wallis test under different stimulation patterns. Under stimulation pattern W1, the inter-group (P-H) significant differences ( $p < 0.05$ ) were observed in slopes values of MNF, RMS, and MAV for biceps brachii and MDF in brachioradialis muscles. However, under W2, significant inter-group (P-H) differences were observed only in slope values of median frequency ( $p < 0.05$ ) for biceps brachii muscle. Under W3, no significant inter-group (P-H) differences were observed in slope values of any myoelectric indices for any muscle.

### B. Trend Analysis

As mentioned in the methods section-M the trend or slope or rate of change of the myoelectric indices was found by using peak values of the myoelectric indices which were linearly fitted to obtain the slope or trend. In FES induced repetitive contractions the myoelectric indices generally decay over cycles during fatigue. Therefore, peak values of myoelectric indices were analyzed. The data spread of peak values of myoelectric indices, measured by standard deviation was high in W1, followed by W2 and W3 as observed in all frequency domain and most time domain indices (as shown in supplementary, Fig. h). The p-values of linear regression (performed on peak values of myoelectric indices) were always less than 0.05 and depicted the significant dependence of peak value of myoelectric indices on cycle number. As observed in supplementary Fig. h, for both biceps brachii and brachioradialis muscles, the peak values of frequency domain myoelectric

indices decreased over cycles with strong and significantly negative correlation ( $r < -0.85$ ,  $p < 0.05$ ). However, the peak values of time domain indices exhibited both positive ( $r > 0.85$ ) and negative ( $r < -0.85$ ) strong and significant correlation ( $p < 0.05$ ) reducing the reliability of time domain indices as fatigue indicators. In Fig. 7 the average slopes of myoelectric indices along with standard deviations are shown for biceps brachii and brachioradialis muscles in post-stroke and healthy participants. It can be observed from Fig. 7, that the slopes of frequency domain fatigue indicators (MNF and MDF) were negative in all cases indicating muscle fatigue [56].

### Part 2 Kinematic Estimator of Performance and Fatigue

### C. Statistical Analysis

It was investigated whether the peak angular displacement per cycle elicited by distinct stimulation patterns in any subject was identical. The myoelectric indices of fatigue are not yet firmly established ways of measuring fatigue in FES evoked intermittent dynamic contractions [49]. Therefore, angle-based [46] and torque-based [45] measurements are mostly used in assessing FES-induced fatigue in dynamic contractions. The peak angular displacement under the three stimulation patterns is shown in Fig. 8 for all subjects (post-stroke as well as healthy participants). The normality of peak angular displacement data generated by a particular stimulation pattern was tested using the Shapiro-Wilk test. The peak angular displacements were normally distributed in all the subjects under all stimulation conditions. Hence, One-Way Repeated Measure Analysis of Variance was used. There were statistically significant differences ( $p < 0.05$ ) in the peak angular displacements generated under the three tested stimulation patterns W1, W2, and W3, indicating that the kinematic output varied significantly under different waveforms for the same elbow flexion activity. To determine the source of the differences, pair-wise comparisons (with Bonferroni correction) on peak angular displacements under distinct stimulation patterns were performed, and the results were shown



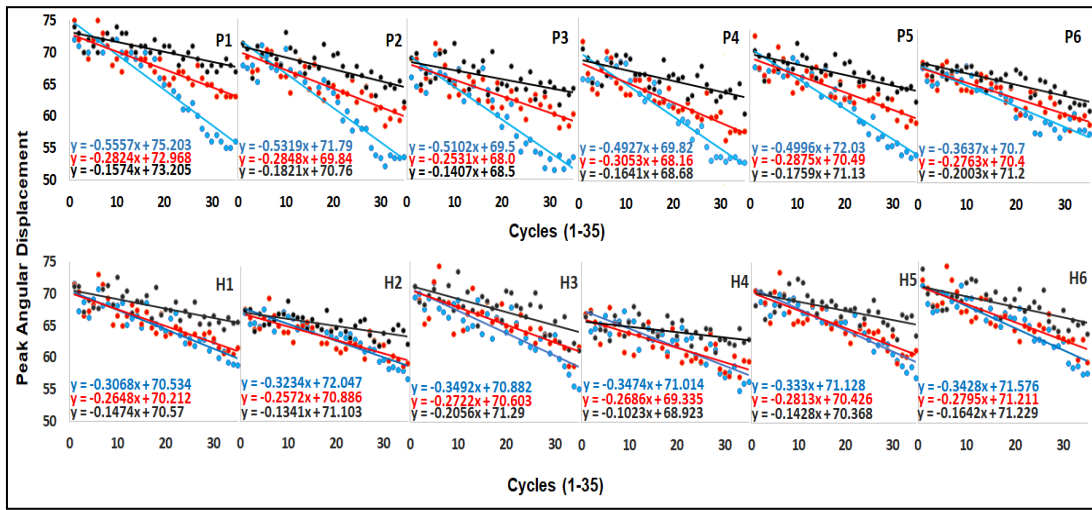


**Fig. 8.** The maximum angular displacements induced by each stimulation pattern cycle-wise is shown in the above figure. Annotations P1-P6 denote post-stroke participants while H1-H6 denote healthy participants. Equations and data points in blue represent customized rectangular stimulation, red represents trapezoidal stimulation pattern while black represents muscle synergy-based stimulation pattern. The black data points are more consistent throughout the cycles than blue and red in both post-stroke and healthy participants showing that kinematic output declined the most in predefined stimulation patterns (denoted in blue and red colors). The p-values of linear regression were found to be less than 0.001 in all cases.

**TABLE II**

ONE-WAY REPEATED MEASURES ANOVA TEST ON PEAK ANGULAR DISPLACEMENTS IN POST-STROKE (P1-P6) AND HEALTHY (H1-H6) PARTICIPANTS (PAIR-WISE COMPARISONS UNDER CONDITIONS- W1(CUSTOMIZED RECTANGULAR STIMULATION PATTERN), W2(TRAPEZOIDAL STIMULATION PATTERN), AND W3(MUSCLE SYNERGY-BASED STIMULATION PATTERN))

	P1	P2	P3	P4	P5	P6	H1	H2	H3	H4	H5	H6
Group1-Group2	P-value	P-value	P-value	P-value	P-value	P-value	P-value	P-value	P-value	P-value	P-value	P-value
W1 - W2	0.02881	0.03236	0.04437	0.38689	0.04437	0.13514	0.45599	0.96899	0.17194	0.93159	0.88165	0.13514
W1 - W3	0.00000	0.00000	0.00000	0.00000	0.00000	0.00000	0.00000	0.00790	0.00001	0.03236	0.00002	0.00000
W2 - W3	0.00070	0.00358	0.00536	0.00038	0.00062	0.00153	0.00062	0.01647	0.01149	0.01149	0.00014	0.00790

in **Table II**. The values highlighted in purple color implies significant differences. From the **Table II** it can be inferred that kinematic output generated during muscle synergy-based stimulation pattern (W3) was different from customized rectangular stimulation pattern (W1) and trapezoidal stimulation pattern (W2). However, there was no statistically significant difference in kinematic output between W1 and W2.

Additionally, the rate of change of peak angular displacement under different stimulation patterns were statistically compared in post-stroke and healthy groups separately. Within the post-stroke group, the statistically significant differences across the stimulation patterns lied between W1-W3 ( $p < 0.0167$ , Bonferroni corrected, the Kruskal Wallis test). For the post-stroke group, slope values under W1 were more negative [-0.5557 to -0.3637] than W3 [-0.2003 to -0.1407]. The same was observed within the healthy group. In the healthy group, slope values under W1 were more negative [-0.3492 to -0.3068] than W3 [-0.2056 to -0.1023].

Since, the experimental design consisted of two groups-healthy and post-stroke. Therefore, it was reasonable to investigate the rate of peak angular displacement decline for these two groups under different stimulation conditions irrespective of inter-subject differences.

**Customized rectangular stimulation pattern:** The slopes of kinematic output decay were compared in healthy and post-stroke participants using Kruskal Wallis test. There was

significant difference in the rate of peak angular displacement decay between healthy and post-stroke participants ( $p < 0.05$ ). From **Fig. 8** it can be observed that the slopes were steeper and more negative (-0.5557 to -0.3637) in post-stroke participants than in healthy participants (-0.3492 to -0.3068) implying a faster rate of kinematic output decline in the former.

**Trapezoidal stimulation pattern:** There was no significant difference in the rate of peak angular displacement decay between healthy and post-stroke participants tested by Kruskal Wallis test ( $p < 0.05$ ). This waveform had a decay rate of (-0.2531 to -0.3053) as per observations in both the groups.

**Muscle synergy-based stimulation pattern:** There was no significant difference in the rate of peak angular displacement decay between healthy and post-stroke participants tested by Kruskal Wallis test ( $p < 0.05$ ). This waveform had a decay rate of (-0.1023 to -0.2056) as per observations in both the groups. So, it can be concluded from **Fig. 8** and above statistical results that customized rectangular waveform worsens the kinematic performance in post-stroke participants the most and is population sensitive which was observable within a small population size.

#### D. Trend Analysis

As depicted in **Fig. 8**, the peak angular displacement values decreased over cycles under all stimulation conditions, but

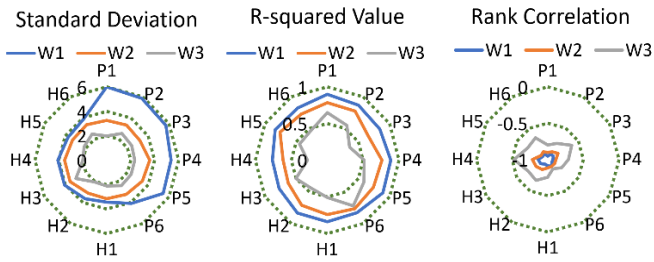


**Fig. 9.** Standard deviation, r-squared value of linear regression, and Spearman's rank correlation values on peak angular displacement data points are shown for all subjects under three different stimulation patterns. The standard deviation was found to be in the order of  $W1 > W2 > W3$ . The r-squared value of linear regression on peak angular displacement was in the order of  $W1 > W2 > W3$ . Similarly, the Spearman's rank correlation was more negative in the order of  $W1 > W2 > W3$ . This analysis indicated that the data consistency/spread was more in muscle-synergy based stimulation pattern (W3), in contrast to customized rectangular pattern (W1) which was steeply declining as evident from highly negative Spearman's rank correlation and high data spread as measured from standard deviation. The outcomes of trapezoidal pattern (W2) lied in middle of the other two patterns (W1 & W3).

the rate of its decline varied. For all participants, this decline was steeper in the customized rectangular stimulation pattern (W1), followed by the trapezoidal (W2) and muscle synergy-based (W3) stimulation patterns, indicating greater fatigue in the former two from the perspective of rate of kinematic output decay (*slopes under W1*  $\in [-0.5557 -0.3086]$ , *slopes under W2*  $\in [-0.3053 -0.2531]$ , and *slopes under W3*  $\in [-0.2056 -0.1023]$ ). From Fig. 9, (a subsequent analysis figure on peak angular displacements data points) the data spread measured by standard deviation was high in W1, followed by W2 and W3. Thus, the obtained values of peak angular displacement were more consistent in W3 followed by W2 and W1. The spearman rank correlation (as shown in Fig. 9) and its p-value, which was always less than 0.001, revealed that there was a significantly strong negative relation between the peak angular displacement and the cycle number in the order  $W1 > W2 > W3$ , implying performance drop in the same order. The p-value of linear regression was less than 0.001 for all subjects under all stimulation patterns, explained that the peak angular displacements significantly depended on the cycle number under all stimulation patterns. This implied that the drop in performance was directly related to increasing cycle numbers. Hence, the type of stimulation pattern directly affected the kinematic performance and fatigue with cyclic progression.

#### IV. DISCUSSION

Muscle synergy-based functional electrical stimulation (FES) has improved muscle coordination in post-stroke patients over the past decade, making it a viable tool for guiding FES patterns in multi-joint activities [15], [16], [17], [18], [19]. Most importantly synergy-based FES solves the problem of "what should be the stimulation template?" Acute benefits of synergy-based FES [15], an automated synergy-based FES [18], and the benefits of a 5-day intervention with synergy-based FES [19] showed possible kinematic and Fugl Meyer score improvements. These findings have encouraged us to translate this stimulation strategy to single-joint activities,

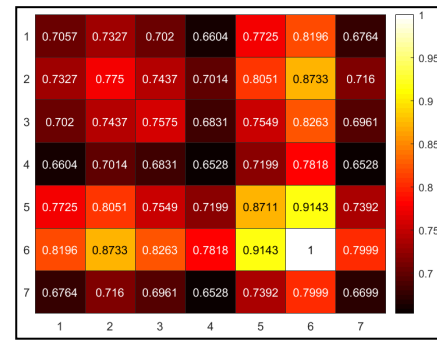


**Fig. 10.** This figure shows the inter-subject similarity of muscle synergies through heat-map. It was found that subject S6 exhibited most similarity with other subjects in terms of muscle synergy, expressible through lighter contrasts in heat-map. Hence, S6 was chosen as the suitable template for driving FES. Each row and column number (1-7) indicate the participant ID of 7 subjects where subject ID of 7 denotes non-paretic arm of post-stroke participant.

where an equal dearth of adequate protocols exists that can be generalized to the patients. The presented work attempts to investigate the possible benefits of synergy-based FES on an important single joint movement- elbow flexion in vertical plane from the perspective of kinematic performance and induced muscle fatigue when compared with traditionally followed stimulation strategies. Single joint movements were targeted because they are crucial for improving joint stability, muscle strength, and functionality in acute and subacute post-stroke conditions. It is also inferred from a previous work [57] that multi-joint synergies are a linear combination of single joint synergies. Hence improving single joint movement synergies could aid in improving multi-joint movements synergies.

However, when it comes to the choice of stimulation template using muscle synergy, a common consensus suggests that the muscle synergies variability is not much pronounced for healthy people and age-matched template could be used [15]. The presented study observed distinct changes in the number of muscle synergies across the participants. The number of synergies specific to biceps curl activity varied from 2 to 3 in healthy participants. Further, in Fig. 10 row 7 of the heat map indicates synergy-similarities of non-paretic limb of post-stroke participant with other participants, which was low. The non-paretic limb of post-stroke participant showed only 1 muscle synergy for biceps curl activity (supplementary Fig. a). Therefore, it posed a major challenge as to whose muscle synergies should be chosen to construct the synergy template as different temporal and weight vectors occurred as shown in supplementary Fig. a. Taking average of synergies become difficult when the obtained synergy numbers vary among participants. Hence, we suggested choosing muscle synergy template from that healthy person who exhibited the least intra- and inter-subject variability in muscle synergy with trials and with other participants respectively. Thus, FES would be driven by a less variable muscle synergy template. Using equation 2, a heat map, Fig. 10, of inter-subject synergistic similarity is shown. This synergy matrix similarity score is useful for comparing synergies of unequal numbers and averaging similarities. Unlike cosine similarity of two vectors, this method does not always return 1 when comparing

the subject to itself. The synergy matrix can contain many vectors, and the average of all vector similarities may be less than 1 for the same subject. It was observed that participant 6 exhibited least intra- and inter- subject variability (*row and column 6 in heat map, Fig. 10*), therefore, muscle synergies from participant 6 were used to drive FES waveforms.

Evoked EMG filtering, a crucial step for post-processing analysis, was highly affected by the choice of filters (*supplementary Fig. b*). Frequency domain filters could often remove the desirable frequencies if administered with less caution. Past work [58] has reported declines in M-wave amplitude (*the main eEMG signal content*) with use of notch filters. Hence, different filters were compared. For example, in one instant the energy content of the raw eEMG signal (*Volt-squared*) was 0.1127, 4 Hz low-pass filtered eEMG signal envelop was 0.0031, EMD-filtered signal was 0.0011, and bandpass-comb was  $9e-5$ . Thus, in the present work, EMD-based filtering yielded more fidelity in terms of preserved signal content, energy, and shape of M-waves (*through visual inspections*) in contrast to blanking window, comb, and bandpass-comb filters which had performed well with singlet pulses in earlier works [43].

The stimulation patterns used in the present study differed in their slope. The rising slope of customized rectangular and trapezoidal waveforms was of the range [1.3125 to 4.0625] and that of muscle synergy-based waveform was [0.9]. The falling slope of customized rectangular was (*-infinity*), that of trapezoidal waveforms was of the range [-1.3125 to -4.0625] and that of muscle synergy-based waveform was [-1.4]. We previously assumed that customized rectangular stimulation might produce the least fatigue since its stimulation duration was shorter (*8 sec. ramp up and 2 sec. hold time*), followed by the other two stimulation patterns, but the results contradicted the assumption. Declining maximum angular displacements produced by this stimulation pattern indicated muscle fatigue.

In healthy and post-stroke participants, the customized rectangular stimulation pattern reduced peak elbow joint angles the most (*Fig. 8*). Through slope values (*Fig. 8*) and Kruskal Wallis test between post-stroke and healthy groups on these (*slope*) values under different stimulation patterns ( $p < 0.05$ ), it was observed that the slope of decline of peak angular displacements was more negative in post-stroke participants ( $-0.5557$  to  $-0.3637$ ) than in healthy participants ( $-0.3492$  to  $-0.3068$ ) under customized rectangular waveform, causing more adverse effects on post-stroke participants. Hence, customized rectangular stimulation patterns were found to be population sensitive in this study.

Trapezoidal stimulation outputs (*range of peak angle decline slope: -0.2531 to -0.3053*) were in between that of customized rectangular (*range of peak angle decline slope: -0.3068 to -0.5557*) and synergy-based patterns (*range of peak angle decline slope: -0.1023 to -0.2056*) and were fatigue-prone too. However, there were no significant differences observed between healthy and post-stroke participants' slope values of peak angular displacements during the application of trapezoidal and muscle synergy-based stimulation waveforms. These two waveforms were not

sensitive to the type of population under the tested sample size.

Performance-wise muscle synergy-based stimulation pattern had the smallest kinematic output decline rate compared to other patterns making it suitable for longer rehabilitation training sessions. These findings are in consensus with outcomes of past work which suggested that conventional methods specifically Trapezoidal stimulation envelopes do not match the biomechanical needs of the tibialis anterior (*TA*) muscle during gait cycle, leading to muscle fatigue and limited walking [13]. It was suggested elsewhere that adding configurable ramp-up and ramp-down durations to the stimulation intensity envelope minimise the detrimental quick tibialis anterior contraction and foot-flap [14].

Within the post-stroke group, the slope of peak angular displacements was significantly more negative in W1 [ $-0.5557$  to  $-0.3637$ ] than W3 [ $-0.2003$  to  $-0.1407$ ] ( $p < 0.0167$ , *Bonferroni corrected, the Kruskal Wallis test*). Similarly, in the healthy group, slope values under W1 were significantly more negative [ $-0.3492$  to  $-0.3068$ ] than W3 [ $-0.2056$  to  $-0.1023$ ] ( $p < 0.0167$ , *Bonferroni corrected, the Kruskal Wallis test*). This implied that the customized rectangular pattern was more adversarial in both healthy and post-stroke groups.

Statistical analysis on distribution of myoelectric indices revealed that indices obtained from synergy-based waveform were significantly different from the other two waveforms (*supplementary Table B*). Same results were observed for statistical analysis on peak values of these myoelectric (*supplementary Table C*). This complements the kinematic findings of *Table II* which highlights that the peak angular displacements obtained in W3 differed from both W1 and W2 stimulation patterns. The peak values in kinematic or myoelectric data were less spread in W3 as compared to W1 and W2 (*Fig. 8 and supplementary Fig. h*) implying output consistency. It was observed that frequency domain myoelectric indices (*MNF and MDF*) were reliable for fatigue estimation in dynamic contractions in this study. These peak values of these indices declined with muscle fatigue [56] during prolonged exercise or repetitive movements in all subjects. For biceps brachii muscle of post-stroke participants, the average slopes of frequency domain myoelectric indices under customized rectangular waveform were more negative ( $-0.19$  and  $-0.19$  for MNF and MDF respectively), indicating more muscle fatigue than synergy-based waveform which had a less negative value ( $-0.15$  and  $-0.1$  for MNF and MDF respectively) for the same. Similar observations held true for brachioradialis muscle as well (*Fig. 7*). In time domain myoelectric indices, the decline of indices was not consistent among participants, like previously reported work [50]. The slope of PTP, MAV and RMS were declining in certain cases but in some cases the slopes increased, leading to inconsistent outcome in time domain (*the positive correlation values can be observed for time domain indices in supplementary Fig. h*). From this study we could infer that the frequency domain indices could be used as estimators of fatigue in FES-induced dynamic contractions alongside kinematic estimators.

FES-induced muscle fatigue in post-stroke patients is affected by— reverse order of size principle of motor

recruitment [59], recruitment of big and nearby electrode fibers [30], non-use of paralyzed muscles and fiber type conversion to fast-twitch fibers [60], and the slope or rate of current injection with distance from surface electrodes [61]. Recently a simulation-based study found that ramping up and down stimulation slopes reduces muscle fatigue [62]. Based on the myoelectric indices observed in present study, it may be postulated that the ramp up and ramp down slopes of current injection might have affected the pattern of recruitment of muscle fibers to observe significant differences ( $p < 0.05$ , *Kruskal Wallis test*) in myoelectric indices of fatigue as well as in peak values of myoelectric indices ( $p < 0.05$ , *Friedman One-Way Repeated Measure Analysis of Variance by Ranks*).

An additional perspective to stimulation induced muscle fatigue can be found from the heat generated in the stimulated muscles. At the end of stimulation, muscle heat rate changes abruptly [63]. The steeper current injection rates cause more muscle heat and a steeper decline in stimulation can reduce the heat dissipation during muscle relaxation, leading to early muscle fatigue [64]. At peak current, most motor units are recruited, and an unexpected de-recruitment may cause improper heat dissipation and muscle fatigue. The slope-dependent stimulations may have induced variable muscle heat which could have led to different rates of unsustained kinematic output under different waveforms. Both customized rectangular and trapezoidal waveforms had steeper current injection, which might have led to more muscular heat accumulation, and sudden/steep current decrease allowed less time for heat to disperse. The muscle synergy-based waveform featured gradual ramp up and ramp down slopes (*Fig. 2*), allowing for heat dissipation and muscle relaxation. Thus, body physiology, fiber type recruitment, injection rate, and stimulation-induced heating of muscles could have altered muscular fatigue in the three waveforms observed in the present study.

In the proposed study, although the results are encouraging, there are still some limitations associated with it that need further investigations. One such limitation is selective stimulation of biceps brachii and brachioradialis muscle which is a subset of muscles that were recorded to extract muscle synergies. The conventional practice followed for elbow flexion stimulated either biceps alone or biceps and brachioradialis together [39] for motion in vertical plane. Biceps brachii, brachioradialis, and brachialis are the prime elbow flexors, however, brachialis being an inner muscle is mechanically disadvantageous to biceps brachii in supinated position and difficult to locate in a paralyzed arm [65], [66], hence, was not stimulated. The stimulation of deltoid anterior and posterior could have given insight on shoulder joint stability which is a limitation as not much could be commented about it. In the presented experiment the shoulder and elbow were positionally maintained using a soft block that blocked the movement/slipping of elbow position.

The extensors -triceps long head and triceps short head were not stimulated as it would have destabilized the elbow joint during vertical motion and could have adversely affected the post-stroke participants who were suffering from flaccidity/floppiness in hand. The preliminary experiments revealed

that stimulating the biceps alone required more current for elbow flexion, but when the synergist muscle brachioradialis was recruited, the current requirement for full flexion decreased supporting the previous findings [67] that synergist stimulation of flexors overcomes the effect of gravity and antagonist's (*extensors'*) partial torque. As a result, both biceps and brachioradialis were activated for full elbow flexion (*Table A in supplementary shows the required stimulation current doses*). Since this work followed conventional protocol of stimulating biceps brachii and brachioradialis and only compared the effects of different stimulation patterns on elbow flexion activity, the study on how the current requirements, kinematic outcomes, and myoelectric outcomes of fatigue might have differed if brachialis (another elbow flexor muscle) would also have been stimulated was not conducted, and this is a limitation of this study. The surrogate outcomes of this study (*sustenance of peak angular displacements and less muscle fatigue in case of muscle synergy-based stimulation pattern*) needs to be validated in a larger sample size with clinically meaningful outcomes (*improvement in Fugl Meyer scores*) in a randomized clinical trial (*RCT*) study design. Long duration study, testing synergy-based FES for other single joint activities, analysing the effect of synergy-based FES on muscular fatigue for multi-joint cases, increasing inclusivity in testing population, all these could further give more insights in understanding the benefits of synergy-based FES. This work does not compare any of its outcomes with multi-joint outcomes of past works [15], [18], [19], as it has not yet been determined what effect muscle synergy-based FES will have on muscular fatigue in multi-joint scenarios.

The current work is an exploratory study, hence, has been done only on a limited number of stroke patients and healthy subjects. In future work, the subject sample with different clinical populations would be made more inclusive and a greater number of subjects would be tested to investigate the rehabilitation outcomes on application of muscle synergy-based stimulation pattern from the perspective of kinematic output and muscular fatigue. An optimization strategy on muscle-synergy based stimulation pattern with any bio-signal feedback can enhance its efficacy which will also be tested in future works. Translation of these templates to single joint movements can serve as reference patterns for clinicians to start with the FES application from the very acute and sub-acute phases.

A possible strategy of implementing synergy-based FES in acute and sub-acute cases where residuary movements are lost, could be by mapping muscle synergy-based reconstructed EMG into FES stimulation pattern by conserving the waveform shape. This could be considered as a differentiator between a synergy-based FES for single joint movement (*this work*) and a previously designed synergy-based FES for multi-joint movement [15], [18].

Methodological advantages of this work are a) choice of muscle synergy for stimulation- an approach was provided for choosing muscle synergy of functional activity, here, single joint elbow flexion for personalizing a synergy template, b) choice of artifact removal strategy from evoked EMG was discussed, and c) synergist muscles' (biceps brachii and

brachioradialis) stimulation strategy for single joint functional activity to reduce maximum current requirement.

## V. CONCLUSION

This study identifies the acute effectiveness of muscle-synergy based stimulation pattern during its application from the perspective of sustaining kinematic output and inducing less muscle fatigue. A comparison of proposed synergy-based FES pattern with existing unguided FES strategies for therapeutic benefits in post-stroke rehabilitation is presented. Synergy-based stimulation pattern was found to be the most effective stimulation pattern for doing repetitive exercises of elbow joint using FES. This study could help in driving long duration FES exercises in clinical setups for maximizing the benefits for post-stroke survivors' movement restoration. This paradigm will be tested on various stroke population groups suffering from paralysis to validate the results and advantages presented in this work. The presented study has potential application in neurological diseases other than stroke like spinal cord injury, Parkinson's, and cerebral palsy. Future work will explore the extension of the present study with larger and varied clinical population.

## REFERENCES

- [1] M. P. Lindsay et al., "World stroke organization (WSO): Global stroke fact sheet 2019," *Int. J. Stroke*, vol. 14, no. 8, pp. 806–817, Oct. 2019, doi: [10.1177/1747493019881353](https://doi.org/10.1177/1747493019881353).
- [2] V. L. Feigin et al., "Update on the global burden of ischemic and hemorrhagic stroke in 1990–2013: The GBD 2013 study," *Neuroepidemiology*, vol. 45, no. 3, pp. 161–176, 2015, doi: [10.1159/000441085](https://doi.org/10.1159/000441085).
- [3] E. Peri et al., "Can FES-augmented active cycling training improve locomotion in post-acute elderly stroke patients?" *Eur. J. Transl. Myol.*, vol. 26, no. 3, p. 6063, Jun. 2016.
- [4] D. G. Everaert, Y. Okuma, V. Abdollah, and C. Ho, "Timing and dosage of FES cycling early after acute spinal cord injury: A case series report," *J. Spinal Cord Med.*, vol. 44, no. 1, pp. S250–S255, Sep. 2021, doi: [10.1080/10790268.2021.1953323](https://doi.org/10.1080/10790268.2021.1953323).
- [5] G. E. Mann, S. M. Finn, and P. N. Taylor, "A pilot study to investigate the feasibility of electrical stimulation to assist gait in Parkinson's disease," *Neuromodulation, Technol. Neural Interface*, vol. 11, no. 2, pp. 143–149, Apr. 2008, doi: [10.1111/j.1525-1403.2008.00157.x](https://doi.org/10.1111/j.1525-1403.2008.00157.x).
- [6] I. Moll et al., "A randomized crossover study of functional electrical stimulation during walking in spastic cerebral palsy: The FES on participation (FESPa) trial," *BMC Pediatrics*, vol. 22, no. 1, pp. 1–15, Jan. 2022, doi: [10.1186/s12887-021-03037-9](https://doi.org/10.1186/s12887-021-03037-9).
- [7] M. Kutlu, C. Freeman, A.-M. Hughes, and M. Spraggs, "A home-based FES system for upper-limb stroke rehabilitation with iterative learning control," *IFAC-PapersOnLine*, vol. 50, no. 1, pp. 12089–12094, Jul. 2017, doi: [10.1016/j.ifacol.2017.08.2153](https://doi.org/10.1016/j.ifacol.2017.08.2153).
- [8] U. Carraro et al., "Biology of muscle atrophy and of its recovery by FES in aging and mobility impairments: Roots and by-products," *Eur. J. Transl. Myol.*, vol. 25, no. 4, p. 221, Aug. 2015, doi: [10.4081/ejtm.2015.5272](https://doi.org/10.4081/ejtm.2015.5272).
- [9] S. Jung, J. H. Bong, S.-J. Kim, and S. Park, "DNN-based FES control for gait rehabilitation of hemiplegic patients," *Appl. Sci.*, vol. 11, no. 7, p. 3163, Apr. 2021, doi: [10.3390/app11073163](https://doi.org/10.3390/app11073163).
- [10] G. M. Lyons, T. Sinkjær, J. H. Burridge, and D. J. Wilcox, "A review of portable FES-based neural orthoses for the correction of drop foot," *IEEE Trans. Neural Syst. Rehabil. Eng.*, vol. 10, no. 4, pp. 260–279, Dec. 2002, doi: [10.1109/TNSRE.2002.806832](https://doi.org/10.1109/TNSRE.2002.806832).
- [11] K. Subramanya, A. J. P. Pinto, M. K. A. Kumar, B. K. Arya, and M. Mahadevappa, "Surface electrical stimulation technology for stroke rehabilitation: A review of 50 years of research," *J. Med. Imag. Health Informat.*, vol. 2, no. 1, pp. 1–14, Mar. 2012.
- [12] D. Tepavac and L. Schwirtlich, "Detection and prediction of FES-induced fatigue," *J. Electromyogr. Kinesiol.*, vol. 7, no. 1, pp. 39–50, 1997, doi: [10.1016/S1050-6411\(96\)00008-9](https://doi.org/10.1016/S1050-6411(96)00008-9).
- [13] G. M. Lyons, D. J. Wilcox, D. J. Lyons, and D. Hilton, "Evaluation of a drop foot stimulator FES intensity envelope matched to tibialis anterior muscle activity during walking," in *Proc. 5th Annu. Conf. Int. Funct. Elect. Stimulation Soc.*, 2000, pp. 448–451.
- [14] L. Vodovnik, M. R. Dimitrijevic, T. Prevec, and M. Logar, "Electronic walking aids for patients with peroneal palsy," in *Proc. Eur. Symp. Med. Electron.*, 1965, pp. 58–61.
- [15] C. M. Niu et al., "Synergy-based FES for post-stroke rehabilitation of upper-limb motor functions," *IEEE Trans. Neural Syst. Rehabil. Eng.*, vol. 27, no. 2, pp. 256–264, Feb. 2019, doi: [10.1109/TNSRE.2019.2891004](https://doi.org/10.1109/TNSRE.2019.2891004).
- [16] V. C. K. Cheung, C. M. Niu, S. Li, Q. Xie, and N. Lan, "A novel FES strategy for poststroke rehabilitation based on the natural organization of neuromuscular control," *IEEE Rev. Biomed. Eng.*, vol. 12, pp. 154–167, 2019, doi: [10.1109/RBME.2018.2874132](https://doi.org/10.1109/RBME.2018.2874132).
- [17] C. Zhuang, J. C. Marquez, H. E. Qu, X. He, and N. Lan, "A neuromuscular electrical stimulation strategy based on muscle synergy for stroke rehabilitation," in *Proc. 7th Int. IEEE/EMBS Conf. Neural Eng. (NER)*, Apr. 2015, pp. 816–819, doi: [10.1109/NER.2015.7146748](https://doi.org/10.1109/NER.2015.7146748).
- [18] C.-H. Chou et al., "Automated functional electrical stimulation training system for upper-limb function recovery in poststroke patients," *Med. Eng. Phys.*, vol. 84, pp. 174–183, Oct. 2020, doi: [10.1016/j.medengphy.2020.09.001](https://doi.org/10.1016/j.medengphy.2020.09.001).
- [19] C. M. Niu et al., "A pilot study of synergy-based FES for upper-extremity poststroke rehabilitation," *Neurosci. Lett.*, vol. 780, May 2022, Art. no. 136621, doi: [10.1016/j.neulet.2022.136621](https://doi.org/10.1016/j.neulet.2022.136621).
- [20] G. Mann, P. Taylor, and R. Lane, "Accelerometer-triggered electrical stimulation for reach and grasp in chronic stroke patients: A pilot study," *Neurorehabilitation Neural Repair*, vol. 25, no. 8, pp. 774–780, Oct. 2011, doi: [10.1177/1545968310397200](https://doi.org/10.1177/1545968310397200).
- [21] L. D. Hedman, J. E. Sullivan, M. J. Hilliard, and D. M. Brown, "Neuromuscular electrical stimulation during task-oriented exercise improves arm function for an individual with proximal arm dysfunction after stroke," *Amer. J. Phys. Med. Rehabil.*, vol. 86, no. 7, pp. 592–596, 2007, doi: [10.1097/PHM.0b013e31806dc0ce](https://doi.org/10.1097/PHM.0b013e31806dc0ce).
- [22] D.-H. Kim and S.-H. Jang, "Effects of mirror therapy combined with EMG-triggered functional electrical stimulation to improve on standing balance and gait ability in patient with chronic stroke," *Int. J. Environ. Res. Public Health*, vol. 18, no. 7, p. 3721, Apr. 2021, doi: [10.3390/ijerph18073721](https://doi.org/10.3390/ijerph18073721).
- [23] R. Tazawa, D. Okano, Y. Hatazawa, and M. Sugi, "Stimulation wave profiles for elbow flexion in surface electrical stimulation based on burst-modulated symmetric biphasic rectangular waves," in *Proc. IEEE Int. Conf. Adv. Robot. Social Impacts (ARSO)*, Oct. 2019, pp. 381–386.
- [24] S. Ferrante et al., "A personalized multi-channel FES controller based on muscle synergies to support gait rehabilitation after stroke," *Frontiers Neurosci.*, vol. 10, p. 425, Sep. 2016, doi: [10.3389/fnins.2016.00425](https://doi.org/10.3389/fnins.2016.00425).
- [25] Y. Li, J. Chen, and Y. Yang, "A method for suppressing electrical stimulation artifacts from electromyography," *Int. J. Neural Syst.*, vol. 29, no. 6, Aug. 2019, Art. no. 1850054, doi: [10.1142/S0129065718500545](https://doi.org/10.1142/S0129065718500545).
- [26] C. Frigo, M. Ferrarin, W. Frasson, E. Pavan, and R. Thorsen, "EMG signals detection and processing for on-line control of functional electrical stimulation," *J. Electromyogr. Kinesiol.*, vol. 10, no. 5, pp. 351–360, Oct. 2000. [Online]. Available: <https://www.elsevier.com/locate/jelekin>
- [27] Y. Zhou, Y. Fang, J. Zeng, K. Li, and H. Liu, "A multi-channel EMG-driven FES solution for stroke rehabilitation," in *Proc. Int. Conf. Intell. Robot. Appl.*, in Lecture Notes in Computer Science: Including Subseries Lecture Notes in Artificial Intelligence and Lecture Notes in Bioinformatics. Cham, Switzerland: Springer Verlag, 2018, pp. 235–243, doi: [10.1007/978-3-319-97586-3\\_21](https://doi.org/10.1007/978-3-319-97586-3_21).
- [28] R. Pilkar et al., "Application of empirical mode decomposition combined with notch filtering for interpretation of surface electromyograms during functional electrical stimulation," *IEEE Trans. Neural Syst. Rehabil. Eng.*, vol. 25, no. 8, pp. 1268–1277, Aug. 2017, doi: [10.1109/TNSRE.2016.2624763](https://doi.org/10.1109/TNSRE.2016.2624763).
- [29] M. K.-L. Chan, R. K.-Y. Tong, and K. Y.-K. Chung, "Bilateral upper limb training with functional electric stimulation in patients with chronic stroke," *Neurorehabilitation Neural Repair*, vol. 23, no. 4, pp. 357–365, May 2009.
- [30] C. Marquez-Chin and M. R. Popovic, "Functional electrical stimulation therapy for restoration of motor function after spinal cord injury and stroke: A review," *Biomed. Eng. OnLine*, vol. 19, no. 1, pp. 1–25, Dec. 2020, doi: [10.1186/s12938-020-00773-4](https://doi.org/10.1186/s12938-020-00773-4).

- [31] Z. Z. Karu, W. K. Durfee, and A. M. Barzilay, "Reducing muscle fatigue in FES applications by stimulating with N-let pulse trains," *IEEE Trans. Biomed. Eng.*, vol. 42, no. 8, pp. 809–817, Aug. 1995, doi: [10.1109/10.398642](https://doi.org/10.1109/10.398642).
- [32] R. Riener and J. Quintern, "A physiologically based model of muscle activation verified by electrical stimulation," *Bioelectrochem. Bioenergetics*, vol. 43, no. 2, pp. 257–264, 1997, doi: [10.1016/S0302-4598\(96\)05191-4](https://doi.org/10.1016/S0302-4598(96)05191-4).
- [33] A. S. P. Sousa et al., "Optimal multi-field functional electrical stimulation parameters for the 'drinking task-reaching phase' and related upper limb kinematics repeatability in post stroke subjects," *J. Hand Therapy*, vol. 35, no. 4, pp. 645–654, Oct. 2022, doi: [10.1016/j.jht.2021.05.002](https://doi.org/10.1016/j.jht.2021.05.002).
- [34] J. Y. Jung, P. S. Youn, and D. H. Kim, "Effects of mirror therapy combined with EMG-triggered functional electrical stimulation to improve on upper extremity function in patient with chronic stroke," *Physikalische Medizin, Rehabilitationsmedizin, Kurortmedizin*, vol. 31, no. 2, pp. 127–135, Apr. 2021, doi: [10.1055/a-1210-2930](https://doi.org/10.1055/a-1210-2930).
- [35] M. F. Rabbi, L. E. Diamond, C. P. Carty, D. G. Lloyd, G. Davico, and C. Pizzolatto, "A muscle synergy-based method to estimate muscle activation patterns of children with cerebral palsy using data collected from typically developing children," *Sci. Rep.*, vol. 12, no. 1, pp. 1–10, Mar. 2022, doi: [10.1038/s41598-022-07541-5](https://doi.org/10.1038/s41598-022-07541-5).
- [36] S. Li, C. Zhuang, C. M. Niu, Y. Bao, Q. Xie, and N. Lan, "Evaluation of functional correlation of task-specific muscle synergies with motor performance in patients poststroke," *Frontiers Neurol.*, vol. 8, p. 337, Jul. 2017, doi: [10.3389/fneur.2017.00337](https://doi.org/10.3389/fneur.2017.00337).
- [37] K. Zhao, Z. Zhang, H. Wen, and A. Scano, "Intra-subject and inter-subject movement variability quantified with muscle synergies in upper-limb reaching movements," *Biomimetics*, vol. 6, no. 4, p. 63, Oct. 2021, doi: [10.3390/biomimetics6040063](https://doi.org/10.3390/biomimetics6040063).
- [38] E. J. Gonzalez, R. J. Downey, C. A. Rouse, and W. E. Dixon, "Influence of elbow flexion and stimulation site on neuromuscular electrical stimulation of the biceps brachii," *IEEE Trans. Neural Syst. Rehabil. Eng.*, vol. 26, no. 4, pp. 904–910, Apr. 2018, doi: [10.1109/TNSRE.2018.2807762](https://doi.org/10.1109/TNSRE.2018.2807762).
- [39] A. Naito, M. Yajima, M. Chishima, and Y.-J. Sun, "A motion of forearm supination with maintenance of elbow flexion produced by electrical stimulation to two elbow flexors in humans," *J. Electromyogr. Kinesiol.*, vol. 12, no. 4, pp. 259–265, Aug. 2002. [Online]. Available: <https://www.elsevier.com/locate/jelekin>
- [40] J. Sanford, J. Moreland, L. R. Swanson, P. W. Stratford, and C. Gowland, "Reliability of the Fugl-Meyer assessment for testing motor performance in patients following stroke," *Phys. Therapy*, vol. 73, no. 7, pp. 447–454, Jul. 1993.
- [41] H. Ring and N. Rosenthal, "Controlled study of neuroprosthetic functional electrical stimulation in sub-acute post-stroke rehabilitation," *J. Rehabil. Med.*, vol. 37, no. 1, pp. 32–36, Jan. 2005, doi: [10.1080/16501970410035387](https://doi.org/10.1080/16501970410035387).
- [42] P. Krause, J. Szecsi, and A. Straube, "FES cycling reduces spastic muscle tone in a patient with multiple sclerosis," *NeuroRehabilitation*, vol. 22, no. 4, pp. 335–337, Oct. 2007.
- [43] Q. Zhang, M. Hayashibe, P. Fraise, and D. Guiraud, "FES-induced torque prediction with evoked EMG sensing for muscle fatigue tracking," *IEEE/ASME Trans. Mechatronics*, vol. 16, no. 5, pp. 816–826, Oct. 2011, doi: [10.1109/TMECH.2011.2160809](https://doi.org/10.1109/TMECH.2011.2160809).
- [44] B. A. C. Osuagwu, E. Whicher, and R. Shirley, "Active proportional electromyogram controlled functional electrical stimulation system," *Sci. Rep.*, vol. 10, no. 1, pp. 1–15, Dec. 2020, doi: [10.1038/s41598-020-77664-0](https://doi.org/10.1038/s41598-020-77664-0).
- [45] E. H. Estigoni, C. Fornusek, R. M. Smith, and G. M. Davis, "Evoked EMG and muscle fatigue during isokinetic FES-cycling in individuals with SCI," *Neuromodulation*, vol. 14, no. 4, pp. 349–355, Aug. 2011, doi: [10.1111/j.1525-1403.2011.00354.x](https://doi.org/10.1111/j.1525-1403.2011.00354.x).
- [46] J. Winslow, P. L. Jacobs, and D. Tepavac, "Fatigue compensation during FES using surface EMG," *J. Electromyogr. Kinesiol.*, vol. 13, no. 6, pp. 555–568, 2003, doi: [10.1016/S1050-6411\(03\)00055-5](https://doi.org/10.1016/S1050-6411(03)00055-5).
- [47] R. Merletti, M. Knaflitz, C. J. de Luca, and C. J. de Luca. (1990). *Myoelectric Manifestations, of Fatigue in Voluntary and Electrically Elicited Contractions*. [Online]. Available: <https://www.physiology.org/journal/jappp>
- [48] R. Merletti, C. J. De Luca, and D. Sathyan, "Electrically evoked myoelectric signals in back muscles: Effect of side dominance," *J. Appl. Physiol.*, vol. 77, no. 5, pp. 2104–2114, Nov. 1994. [Online]. Available: <https://www.physiology.org/journal/jappp>
- [49] M. Ibitoye, E. Estigoni, N. Hamzaid, A. Wahab, and G. Davis, "The effectiveness of FES-evoked EMG potentials to assess muscle force and fatigue in individuals with spinal cord injury," *Sensors*, vol. 14, no. 7, pp. 12598–12622, Jul. 2014, doi: [10.3390/s140712598](https://doi.org/10.3390/s140712598).
- [50] L. R. McKenzie, B. C. Fortune, L. T. Chatfield, and C. G. Pretty, "Evoked electromyographic fatigue indices during intermittent stimulation towards dynamic wrist contractions," in *Proc. ASME Design Eng. Tech. Conf.* New York, NY, USA: American Society of Mechanical Engineers (ASME), 2021, Paper V007T07A009, doi: [10.1115/DETC2021-70962](https://doi.org/10.1115/DETC2021-70962).
- [51] N.-Y. Yu, J.-J. J. Chen, and M.-S. Ju, "Study of the electrically evoked EMG and torque output during the muscle fatigue process in FES-induced static and dynamic contractions," *Basic Appl. Myology*, vol. 9, no. 1, pp. 11–18, 1999.
- [52] J.-J. J. Chen and N.-Y. Yu, "The validity of stimulus-evoked EMG for studying muscle fatigue characteristics of paraplegic subjects during dynamic cycling movement," *IEEE Trans. Rehabil. Eng.*, vol. 5, no. 2, pp. 170–178, Jun. 1997, doi: [10.1109/86.593288](https://doi.org/10.1109/86.593288).
- [53] Z. Li, D. Guiraud, D. Andreu, C. Fattal, A. Gelis, and M. Hayashibe, "A hybrid functional electrical stimulation for real-time estimation of joint torque and closed-loop control of muscle activation," *Eur. J. Transl. Myol.*, vol. 26, no. 3, pp. 193–196, Jun. 2016.
- [54] R. Merletti. (1992). *Electrically Evoked Myoelectric Signals*. [Online]. Available: <https://www.researchgate.net/publication/21592999>
- [55] S. W. Scheff, "Nonparametric statistics," in *Fundamental Statistical Principles for the Neurobiologist*, S. W. Scheff, Ed. New York, NY, USA: Academic, 2016, ch. 8, pp. 157–182, doi: [10.1016/B978-0-12-804753-8.00008-7](https://doi.org/10.1016/B978-0-12-804753-8.00008-7).
- [56] F. B. Stulen and C. J. De Luca, "Frequency parameters of the myoelectric signal as a measure of muscle conduction velocity," *IEEE Trans. Biomed. Eng.*, vol. BME-28, no. 7, pp. 515–523, Jul. 1981, doi: [10.1109/TBME.1981.324738](https://doi.org/10.1109/TBME.1981.324738).
- [57] S. Muceli, A. T. Boye, A. d'Avella, and D. Farina, "Identifying representative synergy matrices for describing muscular activation patterns during multidirectional reaching in the horizontal plane," *J. Neurophysiol.*, vol. 103, no. 3, pp. 1532–1542, Mar. 2010, doi: [10.1152/jn.00559.2009](https://doi.org/10.1152/jn.00559.2009).
- [58] X. Li, W. Z. Rymer, G. Li, and P. Zhou, "The effects of notch filtering on electrically evoked myoelectric signals and associated motor unit index estimates," *J. Neuroeng. Rehabil.*, vol. 8, no. 1, pp. 1–10, Dec. 2011, doi: [10.1186/1743-0003-8-64](https://doi.org/10.1186/1743-0003-8-64).
- [59] C. L. Lynch and M. R. Popovic, "Functional electrical stimulation," *IEEE Control Syst. Mag.*, vol. 28, no. 2, pp. 40–50, Apr. 2008, doi: [10.1109/MCS.2007.914689](https://doi.org/10.1109/MCS.2007.914689).
- [60] E. Lazar, C. Zaldívar, and J. Nicolás, "Functional electrical stimulation (FES) in stroke," University Francisco de Vitoria, Madrid, Spain, 2008. [Online]. Available: <http://hdl.handle.net/10641/374>
- [61] W. M. Grill, "Modeling the effects of electric fields on nerve fibers: Influence of tissue electrical properties," *IEEE Trans. Biomed. Eng.*, vol. 46, no. 8, pp. 918–928, Aug. 1999, doi: [10.1109/10.775401](https://doi.org/10.1109/10.775401).
- [62] E. Noorsal, S. Z. Yahaya, Z. Hussain, R. Bouldville, M. N. Ibrahim, and Y. M. Ali, "Analytical study of flexible stimulation waveforms in muscle fatigue reduction," *Int. J. Electr. Comput. Eng.*, vol. 10, no. 1, pp. 690–703, 2020, doi: [10.11591/ijece.v10i1.pp690-703](https://doi.org/10.11591/ijece.v10i1.pp690-703).
- [63] A. V. Hill, "The heat of shortening and the dynamic constants of muscle," *Proc. Roy. Soc. London B, Biol. Sci.*, vol. 126, no. 843, pp. 136–195, Oct. 1938.
- [64] A. V. Hill, "The mechanism of muscular contraction," *Physiol. Rev.*, vol. 2, no. 2, pp. 310–341, Apr. 1922.
- [65] A. A. Amis, "Chapter 3—Biomechanics of the elbow," in *Operative Elbow Surgery*, D. Stanley and I. A. Trail, Eds. Edinburgh, U.K.: Churchill Livingstone, 2012, pp. 29–44, doi: [10.1016/B978-0-7020-3099-4.00003-5](https://doi.org/10.1016/B978-0-7020-3099-4.00003-5).
- [66] E. W. Brabston, J. W. Genuario, and J.-E. Bell, "Anatomy and physical examination of the elbow," *Operative Techn. Orthopaedics*, vol. 19, no. 4, pp. 190–198, Oct. 2009, doi: [10.1053/j.oto.2009.09.013](https://doi.org/10.1053/j.oto.2009.09.013).
- [67] M. Solomonow, "External control of the neuromuscular system," *IEEE Trans. Biomed. Eng.*, vol. BME-31, no. 12, pp. 752–763, Dec. 1984, doi: [10.1109/TBME.1984.325235](https://doi.org/10.1109/TBME.1984.325235).